

Timelapse Observations Reveal Novel Microbial Mat Dynamics in the Oxygen Minimum Zone of Sur Ridge

Kelly Sonnier, University of Louisiana at Lafayette

Mentors: Steve Litvin, Jim Barry

Summer 2025

Keywords: Deep-Sea Ecology, *Beggiatoa*, Food-Falls, Seasonality

ABSTRACT

Sur Ridge is a deep-sea feature (depth 800-1300 m) within the Monterey Bay National Marine Sanctuary, California, USA. The ridge is a hotspot for biodiversity, especially within its coral and sponge communities, that is partially governed by oceanographic seasons and low oxygen conditions and is an important region for long-term monitoring. From October 2022 to November 2023 the “Mega Coral Cam” timelapse system, deployed near 800m, unexpectedly captured bacterial mats, presumed to be *Beggiatoa* spp., which exhibited a novel form of horizontal migration not previously reported. Images were analyzed in the software ImageJ to measure mat abundance, size, coverage, and speed. Carbon supply was estimated through satellite-derived primary productivity, sediment trap measurements, and gelatinous inputs (pyrosome and larvacean sinkers quantified from the timelapse sequence). Changes in mobile fauna community structure were also estimated from the timelapse. Bacterial mat activity, defined by multiple area metrics, followed seasonal patterns, peaking during the transition between winter storm and upwelling seasons. Mats migrated at ~9.4 cm/week, much slower than previously studied vertical migration rates, which may suggest a different behavior or movement mechanism entirely. Indirect associations with carbon input and a negative correlation with a sea cucumber *Laetmogone* spp. suggest drivers of bacterial mat abundance are complex. This study provides the first evidence of horizontal *Beggiatoa* spp. bacterial mat migration at Sur Ridge, highlighting the need for fine-scale sampling to uncover underlying mechanisms driving their behavior and population dynamics.

INTRODUCTION

Sur Ridge is a geologic feature located ~60 km from Point Sur, with a depth range of 800–1300 meters. It is commonly recognized as a biodiversity hotspot, with over 200 described species (DeVogelaere et. al. 2017). Of these species, abundant coral and sponge gardens provide structure and habitat for mobile fauna, increasing biodiversity of the ecosystem (Girard et. al. 2023). The uppermost portion of the ridge intersects with the oxygen minimum zone (OMZ), which in the California current typically extends from ~500 to 1000 meters depth. Oxygen concentrations in this zone can fall well below average, often less than 1mg/L (Ren et. al. 2025). These hypoxic conditions influence species distributions including the composition of corals, sponges, and their associated fauna across depths.

In addition to low oxygen, Sur Ridge is subject to pronounced seasonality driven by the California current, which plays a role in both coral and sponge physiochemistry as well as associated biodiversity (Girard et. al. 2023). Three primary oceanographic seasons have been described; Upwelling (March-July), when nutrient-rich water enhance productivity; Oceanic (August-October), when warmer surface waters and stratification reduce productivity; and Winter Storm (November-February), when mixing increases productivity, though less than during Upwelling (García-Reyes et. al 2012). The processes governing these seasons directly influence the delivery of organic matter to the seafloor, which in turn, regulates deep-sea benthic activity and community dynamics.

Carbon supply to Sur Ridge occurs through multiple pathways. Particulate organic carbon is produced in the surface ocean through phytoplankton primary productivity and exported to depth, while gelatinous carbon often arrives episodically via food-falls of two organisms. Pyrosomes, colonial tunicates which form large blooms in the upper ocean layers, die off as a group and sink to the sea floor delivering large inputs of both carbon and nitrogen (Lyle et. al. 2022, Archer et. Al. 2018). Larvaceans, solitary free-floating tunicates, release gelatinous nets periodically which trap marine snow while sinking, ultimately transporting both the captured marine snow as well as the carbon and nitrogen from the net itself to the sea floor (Robinson et. al. 2005).

Long-term monitoring is essential for learning more about the specific processes that shape communities at Sur Ridge by providing insight into biological processes that govern their seasonal variability. It also establishes a baseline that may be used to study the effects of climate change, ocean acidification, and industrial practices (e.g. bottom-trawling) on community dynamics. In marine protected areas such as the Monterey Bay National Marine Sanctuary, long-term monitoring data also serves as a management tool for conservation efforts. Technological advances now allow for a non-invasive, high resolution, long-term monitoring of Sur Ridge and other deep-sea habitats.

Beggiatoa spp. (Azeem et. al. 1999), a large filamentous sulfur-oxidizing genus of bacterium, are capable of vertical migration within the sediment. This vertical migration relies on phobic responses to both oxygen in the uppermost layer of sediment and hydrogen sulfide within the lowermost layer (Fig. 1). These physiochemical properties are required for the bacterium's metabolic needs (electron acceptor and electron donor) as well as for the individual filaments' orientation between them. The filaments are able to achieve this by using gliding motility between the layers (Preisler et. al. 2007 ; Dunker et. al. 2011 ; Kamp et. al. 2008). Prior studies have identified *Beggiatoa* spp. and other benthic microbial assemblages as important aspects of the deep-sea carbon cycle (Zhang et. al 2005), making it essential to understand the potential drivers of the microbial dynamics observed at Sur Ridge.

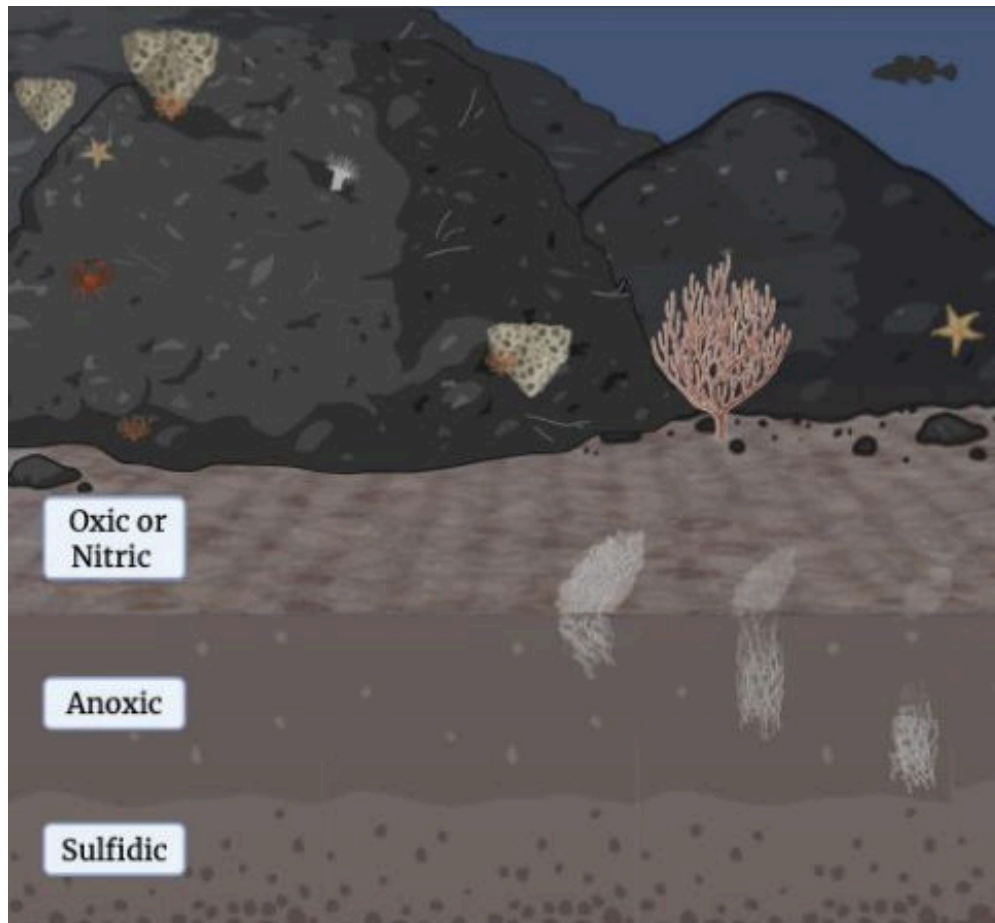


Figure 1. Diagram of *Beggiatoa* spp. movement between sediment layers. *Beggiatoa* spp. receives electrons from the bottommost “Sulfidic” layer, and releases electrons in the uppermost “Oxic or Nitric” layer, their orientation relies on random vertical migration within the “Anoxic” layer. Created in <https://BioRender.com>

The Mega Coral Cam revealed what seem to be mobile microbial mats, which we presume to be *Beggiatoa* spp. (Azeem et. al. 1999). The horizontal migration observed appears distinct from the vertical migration that has been described in most previous work. This previously undocumented behavior may be linked to seasonal food inputs, sediment chemistry, or shifts in carbon availability. Thus, this paper serves as the first description of a novel microbial behavior which aims to address the following questions; [1] How many mats occur throughout the year? [2] At what speed are the bacterial mats migrating? [3] How big are the bacterial mats? [4] How does seasonality, carbon input, mobile macrofauna activity, or a combination of these factors influence these patterns?

DATA COLLECTION

Mega Coral Cam Deployment

The Mega Coral Cam is a timelapse camera system able to provide continuous, direct visual records of benthic communities and their interactions (Girard et al. 2023). The Camera was deployed on October 16, 2022 near the uppermost region of Sur Ridge (Fig. 2), at 863m depth; its position was corrected with ROV Ventana for stability and best view. Taking one image every hour, the camera was able to gather just under 10,000 images before being retrieved in November of 2023.

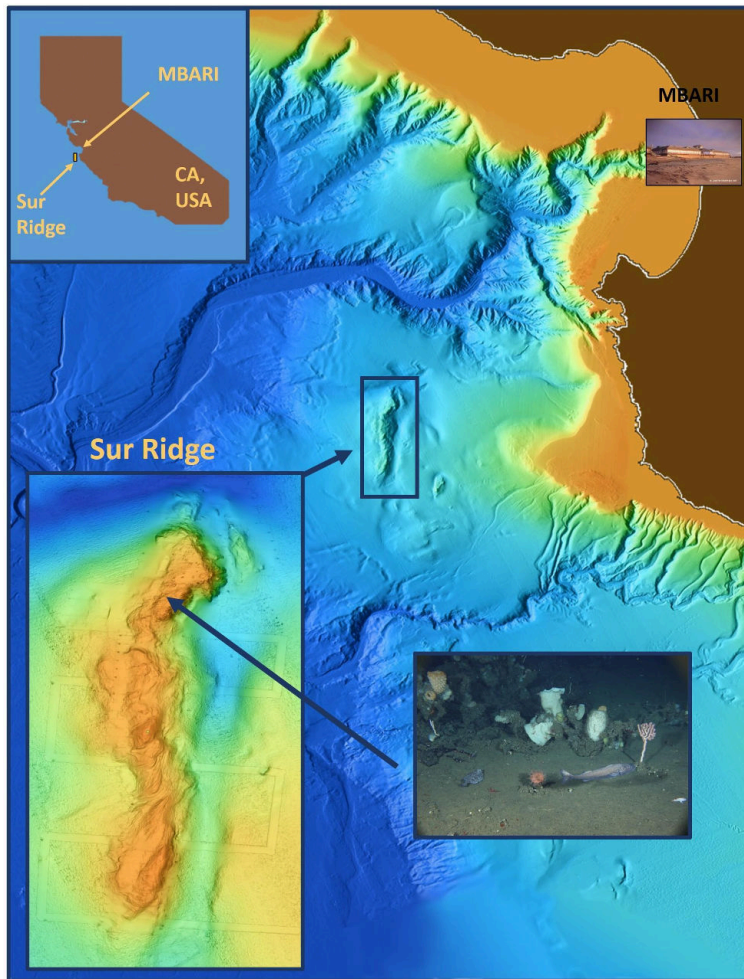


Figure 2. A topographical map of Sur Ridge and site of Mega Coral Cam Deployment.

Bacterial Mat Position and Size

All measurements of mat size and position were conducted using ImageJ photo analysis software. For mat area and migration speed, ROIs were extracted from every 168th image, corresponding to one frame per week. In each image, mats were traced with the ROI (Region of Interest) tool, which provided metrics including area, centroid coordinates, grayscale values, and Feret's length (Fig. 3). To account for changes in camera altitude and angle during the time series, a standard reference point near the center of the image was set as the origin (i.e [0,0], typically in the upper left corner in default ImageJ settings).

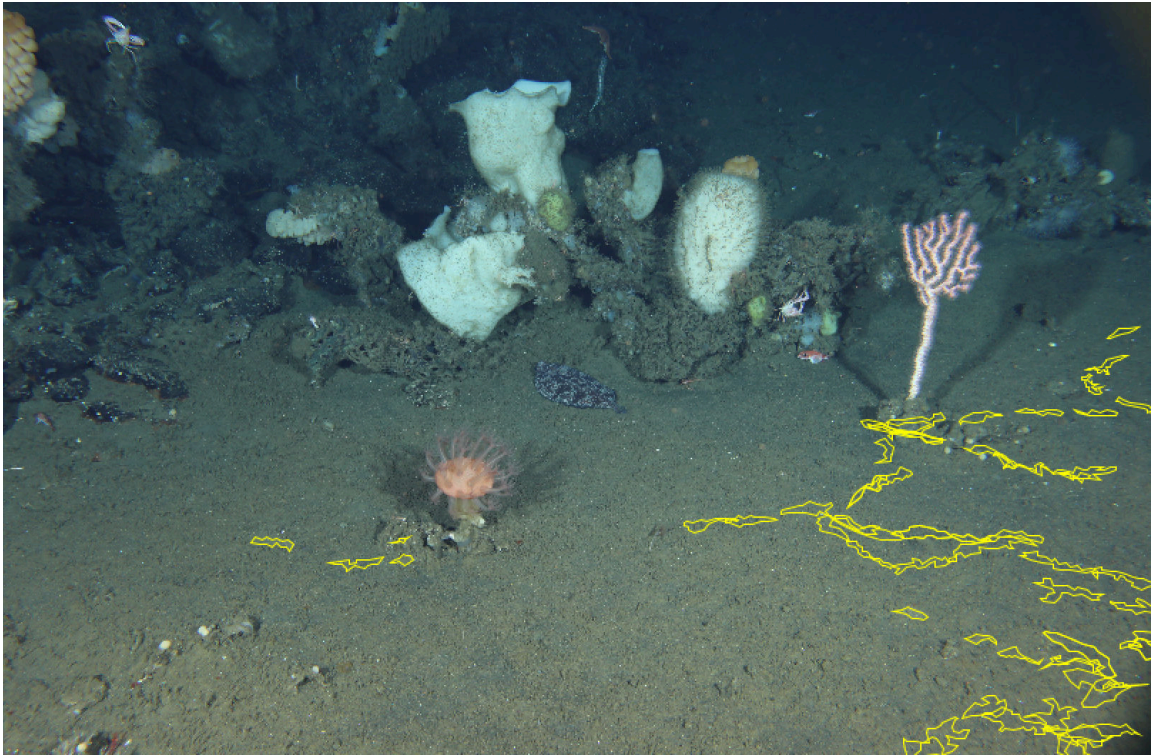


Figure 3. A screenshot of multiple ROIs applied to a given image within the time series using Image J software.

Mobile Community

Images were analyzed twice per week (every ~84 hours). All visible mobile macrofauna were counted and identified to the lowest possible taxonomic level. To focus on taxa most likely to influence bacterial mat dynamics, data on four groups were analyzed separately (see below) based on their high abundance and strong temporal variation: *Laetmogone* spp. (sea cucumbers), *Munida quadrispina* (squat lobsters), *Chorilia longipes* (longhorn decorator crabs), and Asteroidea (sea stars). These taxa were considered the most relevant for evaluating potential interactions with bacterial mats through grazing pressure and bioturbation, although only indirect or complex drivers of mat dynamics were anticipated.

Carbon Inputs

Two metrics of particulate carbon input were analyzed in this study. The first was satellite-derived estimates of phytoplankton primary productivity within a 50×50 km area above Sur Ridge which were calculated using the Vertically Generalized Production Model algorithm, based on satellite-derived MODIS Chlorophyll-a concentration data and available light and temperature-dependent photosynthetic efficiency (Ocean Productivity Website, <https://orca.science.oregonstate.edu/index.php>). To assess how much of this exported carbon reached the seafloor, data from a sediment trap positioned approximately 15 m above Sur Ridge were also examined. Particulate carbon input was expected to serve as a primary, direct driver of microbial mat dynamics. Two additional sources of carbon to the benthic ecosystem, here referred to as gelatinous carbon, consisting of: [1] pyrosomes, large colonial tunicates that sink to the seafloor, and [2] discarded larvacean houses, or “sinkers.” Both were counted using a compiled video that combined all timelapse images into a continuous sequence. While these inputs contribute to the trophic structure of Sur Ridge, direct effects on microbial mat activity were not expected.

DATA ANALYSIS

A Canadian (perspective) grid was applied to correct for size distortion in angled seafloor images (Wakefield & Genin, 1987). The grid was generated from camera focal length, resolution, and angle to the seabed. Because objects appear smaller farther from the camera, the grid scales cell sizes so that measurements of distance and area match true seafloor values (Fig. 4).

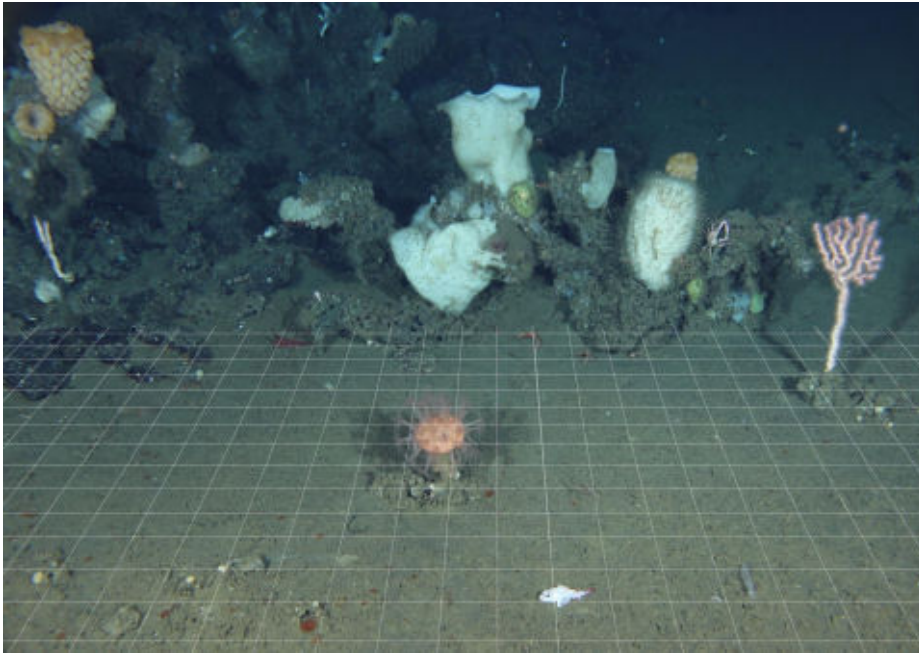


Figure 4. A screenshot demonstrating the Canadian grid overlay on a given image within the time series.

Using this grid, mat outlines were converted into surface areas and centroid positions expressed in centimeters. When first appearing in the time series a bacterial mat was given a unique identity to avoid recounts and track individual variation. Centroid locations from weekly images were compared to calculate movement speed, defined as the path length between two sequential centroids of a given bacterial mat, converted from pixels to cm using the Canadian Grid.

Mat size was calculated by the transformed (i.e. pixels to cm^2) area data gathered on Image J. Average mat size was calculated by dividing the sum of mat areas in a given week by the abundance. This was averaged per month based on the number of weeks/pictures analyzed in this month. Average mat coverage represents the sum of mat areas in a given image, averaged for each month respectively, this is represented with an extra axis depicting the percent coverage, which was calculated by dividing the coverage by the total available area.

Frequently bacterial mats were observed entering and exiting out of frame, during which the entirety of the mat was not visible. To avoid underestimation, only measurements of mats when fully visible within the frame were used in mat area estimations. Other obstacles such as shadows and mobile megafauna could obstruct mat visibility and on these occasions area measurements excluded in subsequent analysis. Monthly mat abundance was quantified by measuring the amount of unique bacterial mats in a given month, where each mat was given an identifier to avoid miscounts. To visualize seasonality trends, all temporal data were graphed with a color palate reflecting the three oceanographic seasons (Fig. 5).

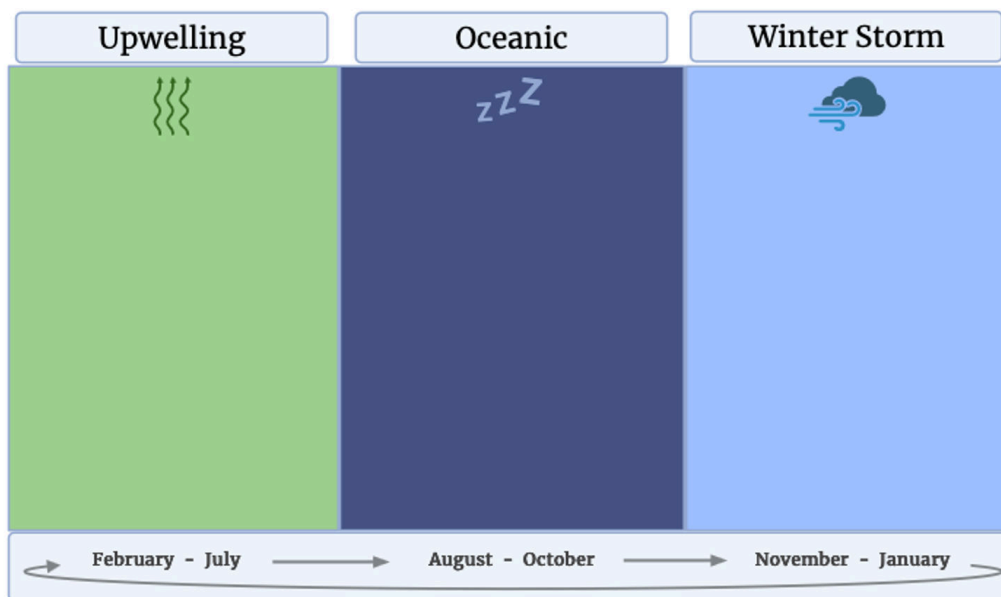


Figure 5. Color-scheme used to represent the three oceanic seasons as described by García-Reyes et. al 2012. Created in www.BioRender.com

All mobile community abundance data were Hellinger-transformed to normalize variability. Community similarity was evaluated using the Bray–Curtis similarity index, and relationships between community composition and time were assessed with a Mantel test. Patterns in community structure were visualized with a non-metric multidimensional scaling (NMDS) ordination, and environmental fit (envfit), based on species abundance, regression vectors were added to visualize species' influence. Abundance of *Laetomogone spp.* was also analyzed separately due to its role as a deposit feeder. All data was analyzed using R Studio version 4.5.1.

RESULTS

Monthly mat abundance, the number of unique bacterial mats present within a given month, exhibited a fourfold range (Fig. 6) with an overall mean of 3.3. Abundance was initially low, rising at the transition from the oceanic to winter storm periods in early 2023, and peaking in the early upwelling season before returning to approximate mean levels until the oceanic season later that year, where they dropped to lowest seen in this study. Weekly mat speed varied widely, from <1 to over 20 cm/week (mean 9.4, SD 3.73), though exhibited no seasonal patterns (Fig. 7).

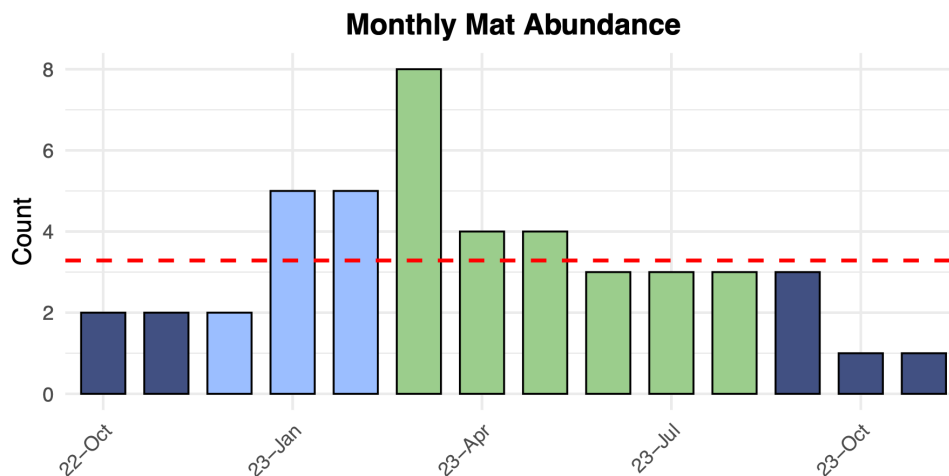


Figure 6. A bar plot representing the count of unique mat identities within a given month with a red dotted line representing the mean abundance.

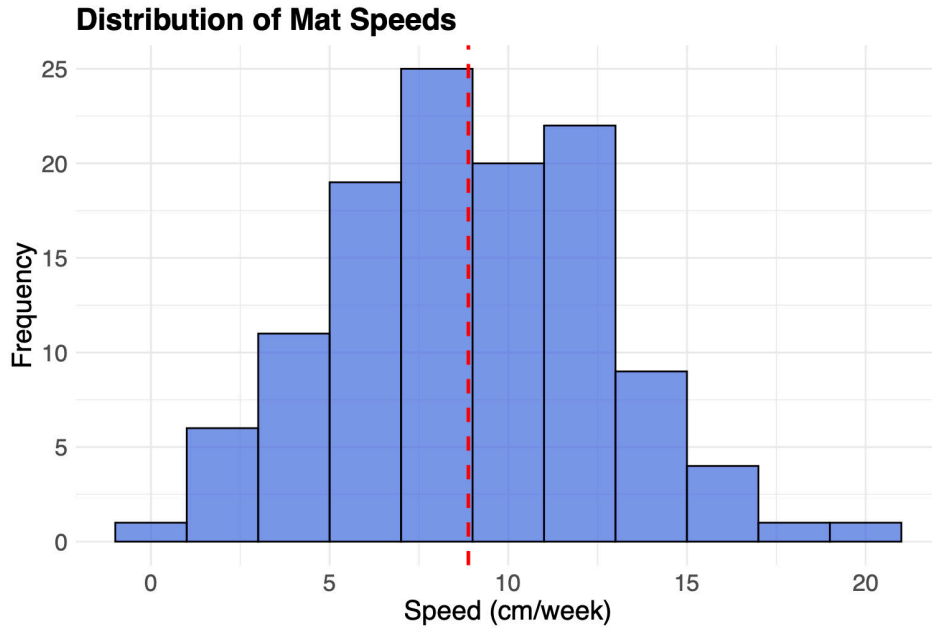


Figure 7. A histogram demonstrating the distribution of bacterial mat speeds measured in cm/week, the red dotted line represents the average speed across all measurements taken.

The distribution of mat sizes (i.e. measurements of all mats across the entire timeseries) was wide (Fig. 8) with a maximum of over 30cm². Pooled by month, mat sizes were initially small during the early oceanic season, increased through the winter storm period, reached a maximum during the transition into upwelling, and then decreased as oceanic conditions returned (Fig. 9). Total monthly mat coverage (Fig.10), the total area covered by all mats for each month, had a mean of 20 cm² and reflected the similar seasonal patterns of mat abundance and size with low coverage in the initial oceanic season, increasing through winter storms, peaking at the winter storm–upwelling transition, and declining toward the end of the time series.

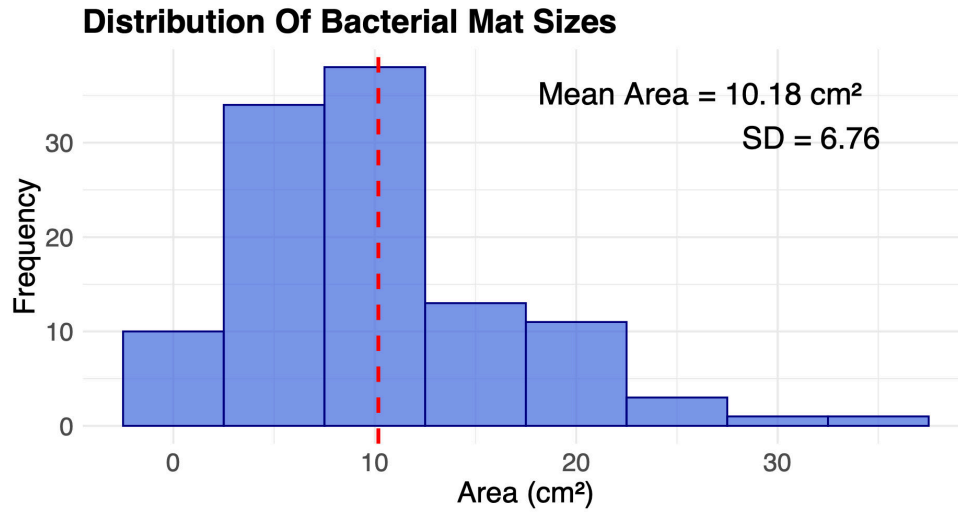


Figure 8. Histogram of bacterial mat sizes (cm²). Red dotted line represents the average size across all measurements taken.

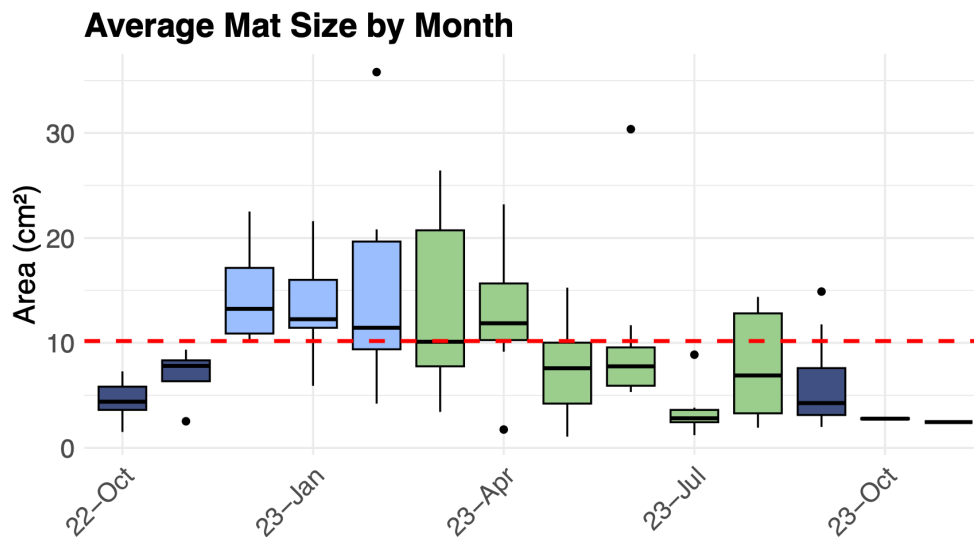


Figure 9. Box plot of monthly average mat size. Red dotted line denotes the average size taken across all measurements (10.18 ± 6.76 cm²).

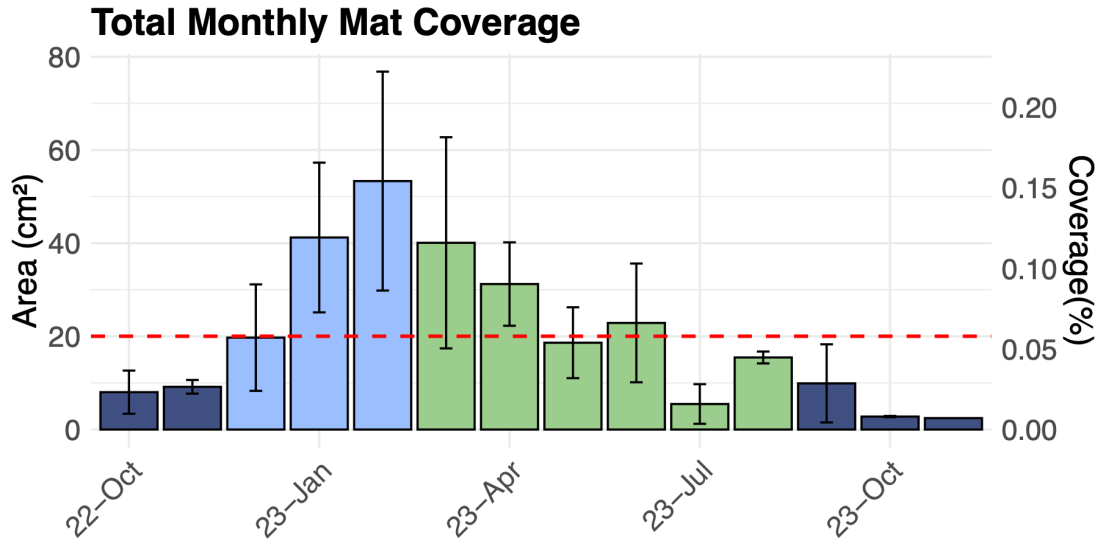


Figure 10. Bar plot of total mat coverage expressed both as cm² as well as percent coverage of available seabed (weekly total mat coverage/area of total possible available seabed * 100) averaged by month. The red dotted line represents the average mat coverage across all measurements taken.

Particulate carbon input (Fig. 11a), measured from both satellite estimates of phytoplankton productivity and sediment trap data, peaked during the upwelling season. These peaks occurred at the same time, with no clear lag between surface production and the arrival of particles at the seafloor. Gelatinous carbon inputs (Fig. 11b) showed different temporal patterns relative to means of particulate organic matter. Pyrosome falls had peaks at both the start and end of the upwelling season but did not appear to match changes in mat coverage. Larvacean sinkers, on the other hand, peaked early in the time series during the oceanic season and then declined.

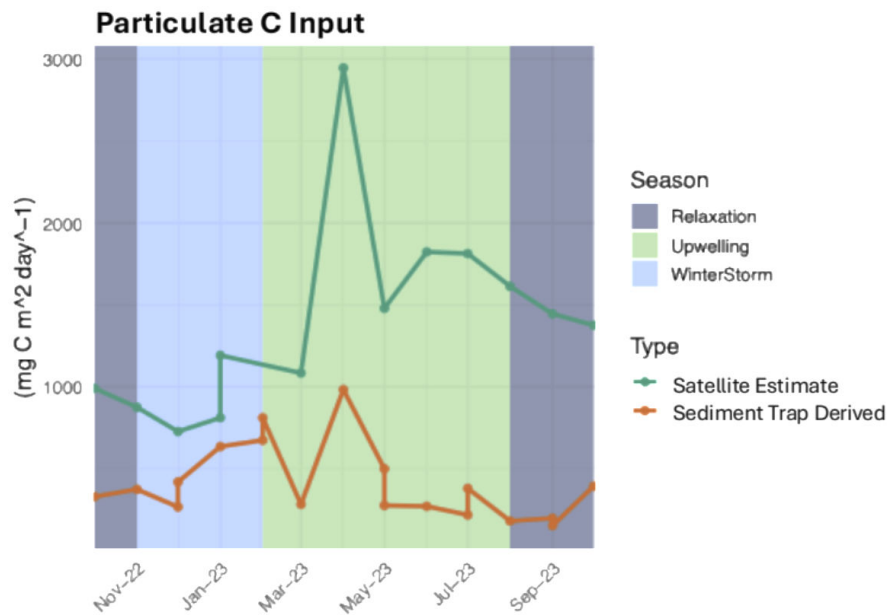


Figure 11a. Particulate carbon estimation from satellite derived phytoplankton primary productivity as well as captured by sediment traps ~15m above the top of Sur Ridge (mg C/m²/day).

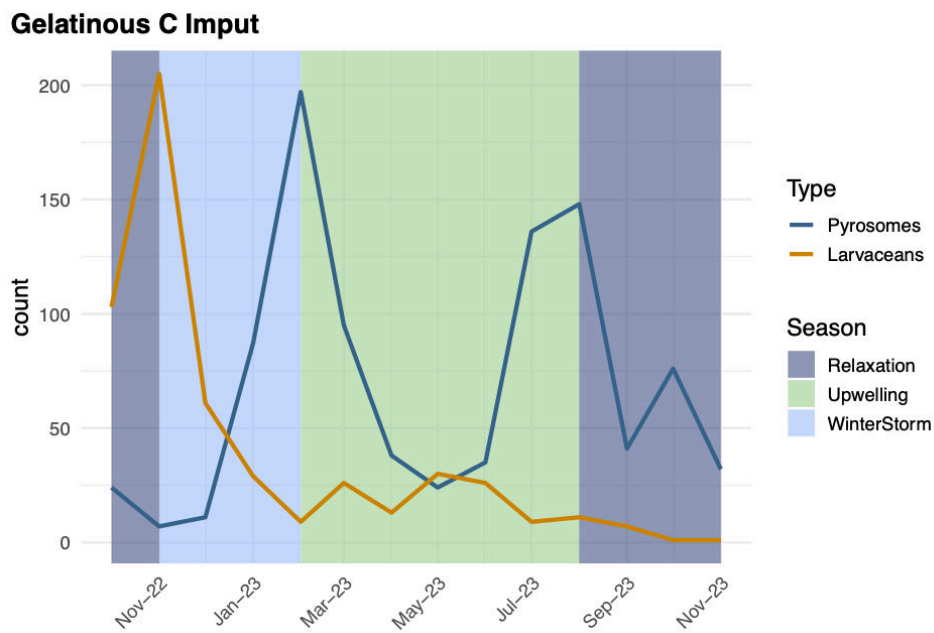


Figure 11b. Gelatinous carbon input as counts taken of both pyrosome and larvacean houses during the time series.

Mobile fauna abundance (Fig. 12) showed no consistent pattern with respect to mat activity or oceanographic season. A negative correlation was observed with the abundance of the deposit-feeding sea cucumber *Laetmogone* spp. only (Fig. 13). Community composition shifted slightly (Mantel; $r = 0.1724$), but significantly ($p < 0.05$) over time (Fig. 14), with decreasing *Munida quadrispina* and increasing Asteroidea abundance across the timeseries.

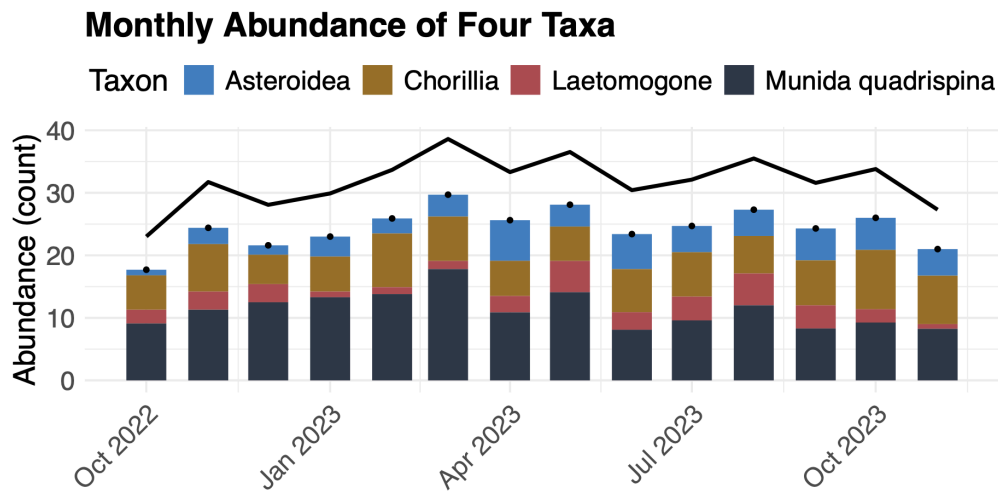


Figure 12. Bar plot showing total monthly count of mobile megafauna observed over the time series with a smoothed line to demonstrate the general pattern (lm).

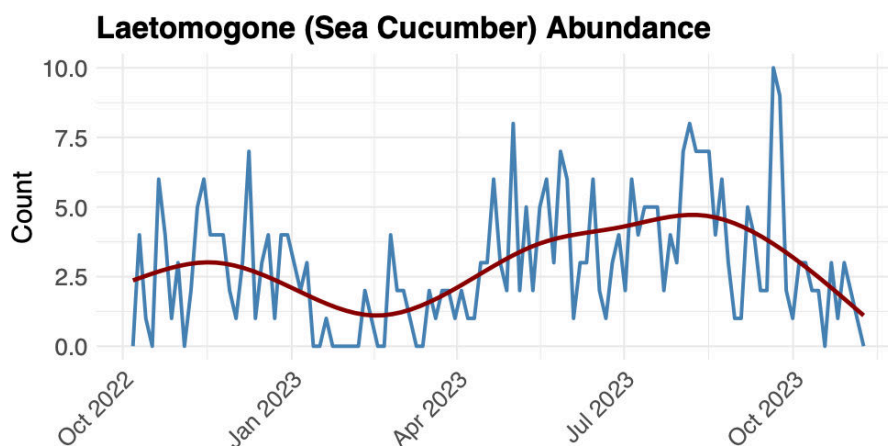


Figure 13. Line graph of the biweekly abundance of *Laetmogone* spp., a deep-sea sea-cucumber. Curve fit is a loess locally weighted mean.

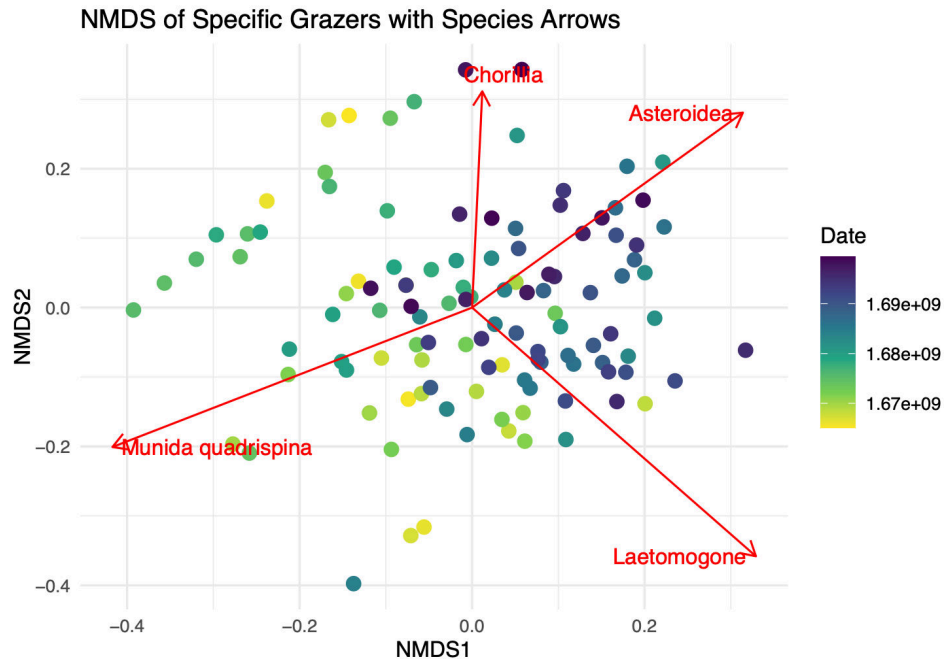


Figure 14. A 2D NMDS demonstrating the change in community composition throughout the timeseries with added species vectors (envfit).

DISCUSSION

Mat Speed, Size and Abundance

In vitro studies of vertical migration have demonstrated *Beggiatoa* filaments can glide vertically at $\sim 2\text{--}4\ \mu\text{m/s}$, equivalent to approximately 120–240 cm per week (Jørgensen et al., 2010; Hinck et al., 2007). While it is possible that our average measurement of speed is underestimated, the vast difference in mean speeds supports the idea that the observed activity is a different type of migration entirely. The relatively slow mat speeds measured here, compared with faster rates reported for vertical migration, suggest that a different type of movement is occurring. This slower pattern may reflect localized growth and death rather than coordinated migration, but confirming this would require closer investigation using microscopy or sediment sampling.

Seasonality appears to be a useful predictor of mat activity, reflected in this study via patterns mat in abundance, size, and coverage, which all peak in the transition between the ocean storm and upwelling seasons. This could be the result of heightened

productivity, however our estimations of carbon input point to complex or indirect drivers. The change in current speeds and patterns associated with seasonal shifts may affect sediment properties (Fig. 1) in such a way that influences mat activity (e.g. shear stress). It is possible that the size variation in individual mats over time may represent physical modulation of metabolism; mats may decrease surface area in the absence of resources to limit the transfer of electrons, and vice-versa. The increase in overall mat coverage (Fig. 10) may support this proposed metabolic strategy, however the simultaneous increase in size variation may speak more favorably to a response in sediment properties.

Role of Carbon Inputs

Particulate carbon input (Fig. 11a), measured from both satellite estimates of phytoplankton productivity and sediment trap data, peaked during the upwelling season. These peaks occurred at the same time, with no clear delay between surface production and the arrival of particles at the seafloor. This was unexpected, since sinking particles are usually thought to take time before reaching depth. Gelatinous carbon inputs (Fig. 11b) showed different temporal patterns relative to means of particulate organic matter. Pyrosome falls had peaks at both the start and end of the upwelling season but did not appear to match changes in mat coverage. Larvacean sinkers, on the other hand, peaked early in the time series during the oceanic season and then declined. Because this pulse came before increases in mat activity, larvacean inputs may influence the conditions that allow mats to grow, though their effects are likely indirect. Overall, the timing of particulate and gelatinous carbon inputs compared to mat coverage suggests that carbon delivery may shape mat dynamics in complex or indirect ways, interacting with seasonal changes in the water column, benthic animals, and sediment conditions.

Mobile Community

The changes observed in mobile macrofaunal community abundance over time, specifically *Laetmogone spp.*, suggests that mobile activity, such as bioturbation or grazing, may alter the sediment conditions needed by *Beggiatoa spp.* (Fig. 1) to thrive. Sea cucumbers are recognized as sediment engineers that can strongly influence seafloor properties (Miller et al., 1988), so a relationship between their abundance and mat presence is reasonable to expect. The broader mobile fauna community also changed over time, influenced in part by shifts in individual species (Fig. 14), but these changes could not be directly linked to mat activity.

CONCLUSIONS and RECOMMENDATIONS

Bacterial mats at Sur Ridge exhibited clear seasonal patterns in abundance, size, and overall coverage, peaking during the winter storm and upwelling seasons and declining afterward. While no single direct driver was identified, several indirect relationships emerged. Particulate carbon inputs from surface productivity and sediment traps peaked during the upwelling season but did not align precisely with mat coverage. Gelatinous inputs showed different dynamics, with larvacean sinkers peaking earlier in the time series and potentially influencing conditions for mat development, while pyrosome falls showed no clear connection. A negative correlation was observed with the deposit-feeding sea cucumber *Laetmogone spp.*, a known sediment engineer capable of altering sediment properties through bioturbation and grazing. Broader shifts in the mobile fauna community were documented, though interesting as standalone results, they did not show consistent links to microbial mat activity. The movement of mats in the time series remains unresolved. Slow speeds compared with reported vertical migration rates suggest that expansion may reflect localized growth at mat edges with die-off elsewhere, rather than coordinated migration of entire mats. To better understand these dynamics, future research should pair time-lapse imaging with sediment cores, microsensor profiling, and microbial sampling to link mat behavior with sediment properties and microbial processes.

ACKNOWLEDGEMENTS

I would like to thank my mentors, Jim Barry and Steve Litvin, for their guidance and expertise throughout this project, as well as the members of the Seafloor Ecology Lab, my desk buddy, Shimeng Zhu for her humor and encouragement, Lonny Lundsten for his ideas and support, the organizers and supporters of the MBARI Internship program, especially George Matsumoto, Megan Bassett, and Jessica Chapman. Finally, big ups to my cohort, housemates, and everyone else who helped make this summer so outstanding.

The MBARI Summer Internship Program is generously supported through a gift from the Dean and Helen Witter Family Fund and the Rentschler Family Fund in memory of former MBARI board member Frank Roberts (1920-2019) and by the David and Lucile Packard Foundation. Additional funding is provided by the Maxwell/Hanrahan Foundation.

References:

Ahmad, Azeem, James P. Barry, and Douglas C. Nelson. 'Phylogenetic Affinity of a Wide, Vacuolate, Nitrate-Accumulating *Beggiatoa* Sp. from Monterey Canyon, California, with *Thioploca* Spp.' *Applied and Environmental Microbiology* 65, no. 1 (1999): 270–77.

Archer, Stephanie K., Amanda S. Kahn, Sally P. Leys, et al. 'Pyrosome Consumption by Benthic Organisms during Blooms in the Northeast Pacific and Gulf of Mexico'. *Ecology* 99, no. 4 (2018): 981–84.
<https://doi.org/10.1002/ecy.2097>.
<https://doi.org/10.1128/aem.65.1.270-277.1999>.

Buhl-Mortensen, Lene, Ann Vanreusel, Andrew J. Gooday, et al. 'Biological Structures as a Source of Habitat Heterogeneity and Biodiversity on the Deep Ocean Margins'. *Marine Ecology* 31, no. 1 (2010): 21–50.
<https://doi.org/10.1111/j.1439-0485.2010.00359.x>.

- Dunker, Rita, Hans Røyne, Anja Kamp, and Bo Barker Jørgensen. 'Motility Patterns of Filamentous Sulfur Bacteria, *Beggiatoa* Spp.' *FEMS Microbiology Ecology* 77, no. 1 (2011): 176–85. <https://doi.org/10.1111/j.1574-6941.2011.01099.x>.
- Edmonds, Caroline. *Seasonality of the Deep Sea ~ Bamboo Corals*. n.d.
- García-Reyes, M., and J. L. Largier. 'Seasonality of Coastal Upwelling off Central and Northern California: New Insights, Including Temporal and Spatial Variability'. *Journal of Geophysical Research: Oceans* 117, no. C3 (2012). <https://doi.org/10.1029/2011JC007629>.
- Girard, Fanny, David W. Caress, Jennifer B. Paduan, et al. 'Habitat Heterogeneity over Multiple Scales Supports Dense and Diverse Megafaunal Communities on a Northeast Pacific Ridge'. *Limnology and Oceanography* 70, no. 2 (2025): 377–92. <https://doi.org/10.1002/lno.12766>.
- Girard, Fanny, Steven Y. Litvin, Alana Sherman, et al. 'Epibenthic Faunal Community Dynamics and Seasonal Species Turnover in a Deep-Sea Coral Ecosystem'. *Deep Sea Research Part I: Oceanographic Research Papers* 196 (June 2023): 104048. <https://doi.org/10.1016/j.dsr.2023.104048>.
- Hinck, Susanne, Marc Mussmann, Verena Salman, et al. 'Vacuolated *Beggiatoa*-like Filaments from Different Hypersaline Environments Form a Novel Genus'. *Environmental Microbiology* 13, no. 12 (2011): 3194–205. <https://doi.org/10.1111/j.1462-2920.2011.02513.x>.
- Jørgensen, Bo Barker, Rita Dunker, Stefanie Grünke, and Hans Røy. 'Filamentous Sulfur Bacteria, *Beggiatoa* Spp., in Arctic Marine Sediments (Svalbard, 79°N)'. *FEMS Microbiology Ecology* 73, no. 3 (2010): 500–513. <https://doi.org/10.1111/j.1574-6941.2010.00918.x>.

- Kamp, Anja, Hans Røy, and Heide N. Schulz-Vogt. 'Video-Supported Analysis of Beggiatoa Filament Growth, Breakage, and Movement'. *Microbial Ecology* 56, no. 3 (2008): 484–91. <https://doi.org/10.1007/s00248-008-9367-x>.
- Lyle, Joanna T, Robert K Cowen, Su Sponaugle, and Kelly R Sutherland. 'Fine-Scale Vertical Distribution and Diel Migrations of *Pyrosoma Atlanticum* in the Northern California Current'. *Journal of Plankton Research* 44, no. 2 (2022): 288–302. <https://doi.org/10.1093/plankt/fbac006>.
- Maritan, Andrew J, Cody S Clements, Zoe A Pratte, Mark E Hay, and Frank J Stewart. 'Sea Cucumber Grazing Linked to Enrichment of Anaerobic Microbial Metabolisms in Coral Reef Sediments'. *The ISME Journal* 19, no. 1 (2025): wraf088. <https://doi.org/10.1093/ismejo/wraf088>.
- Preisler, André, Dirk de Beer, Anna Lichtschlag, Gaute Lavik, Antje Boetius, and Bo Barker Jørgensen. 'Biological and Chemical Sulfide Oxidation in a Beggiatoa Inhabited Marine Sediment'. *The ISME Journal* 1, no. 4 (2007): 341–53. <https://doi.org/10.1038/ismej.2007.50>.
- Ren, A. S., D. L. Rudnick, and D. P. Nicholson. 'Seasonal Dissolved Oxygen Gas Exchange in the California Current Upwelling System'. *Progress in Oceanography* 236 (August 2025): 103473. <https://doi.org/10.1016/j.pocean.2025.103473>.
- ResearchGate. '(PDF) Sur Ridge Field Guide: Monterey Bay National Marine Sanctuary'. Accessed 20 August 2025. https://www.researchgate.net/publication/320716655_Sur_Ridge_Field_Guide_Monterey_Bay_National_Marine_Sanctuary.
- Robison, Bruce H., Kim R. Reisenbichler, and Rob E. Sherlock. 'Giant Larvacean Houses: Rapid Carbon Transport to the Deep Sea Floor'. *Science (New York, N.Y.)* 308, no. 5728 (2005): 1609–11. <https://doi.org/10.1126/science.1109104>.

- Schwedt, Anne, Anne-Christin Kreutzmann, Lubos Polerecky, and Heide N. Schulz-Vogt. 'Sulfur Respiration in a Marine Chemolithoautotrophic Beggiatoa Strain'. *Frontiers in Microbiology* 2 (January 2012): 276. <https://doi.org/10.3389/fmicb.2011.00276>.
- Wakefield, W. Waldo, and Amatzia Genin. 'The Use of a Canadian (Perspective) Grid in Deep-Sea Photography'. *Deep Sea Research A* 34 (March 1987): 469–78. [https://doi.org/10.1016/0198-0149\(87\)90148-8](https://doi.org/10.1016/0198-0149(87)90148-8).
- Zhang, Chuanlun L., Zhiyong Huang, James Cantu, et al. 'Lipid Biomarkers and Carbon Isotope Signatures of a Microbial (Beggiatoa) Mat Associated with Gas Hydrates in the Gulf of Mexico'. *Applied and Environmental Microbiology* 71, no. 4 (2005): 2106–12. <https://doi.org/10.1128/AEM.71.4.2106-2112.2005>.